Biophysical Journal, Volume 98

Supporting Material

The Interaction of αB-Crystallin with Mature α-Synuclein Amyloid Fibrils Inhibits their Elongation

Christopher A Waudby, Tuomas P. J. Knowles, Glyn L. Devlin, Jeremy N. Skepper, Heath Ecroyd, John A. Carver, Mark E. Welland, John Christodoulou, Christopher M. Dobson, and Sarah Meehan

The Interaction of αB-Crystallin with Mature α-Synuclein Amyloid Fibrils Inhibits their Elongation: Supporting Material

Materials and Methods

Unless otherwise stated, all chemicals were purchased from Sigma-Aldrich (UK). Thioflavin T (ThT) was supplied at 67% purity, and may contain hydrophobic contaminants that have a significant effect on aggregation reactions. Therefore, prior to use the crude solid was dissolved in tetrahydrofuran and pure ThT was recovered by filtration. This procedure was repeated three times, and the final solid was dried under reduced pressure. αB-Crystallin was expressed and purified according to previously published protocols (1). The A53T αSyn construct was prepared in a pT7-7 vector by site-directed mutagenesis of the WT using a Stratagene QuikChange kit, and was then expressed and purified as described previously (2).

Preparation of αSyn fibrils

To obtain a high quality preparation of fibrils with minimal amounts of amorphous material, it proved necessary to grow two generations of fibrils, termed 'F0' and 'F1': in our hands, direct (unseeded) preparations of αSyn fibrils contained significant quantities of amorphous material (Fig. S5*A*). F0 fibrils were prepared from a solution of 70 μM A53T αSyn in 500 μL of PBS (10 mM sodium phosphate pH 7.5, 100 mM sodium chloride and 0.1% sodium azide). This solution was passed through a 0.22 μm syringe filter into a clean, sterile 2 mL Eppendorf tube containing a small, teflon-coated magnetic stirrer bar, and incubated at 310 K for 24 hr with vigorous stirring. The visibly turbid solution thus formed was centrifuged for 30 min at $16000 \times g$, the supernatant was discarded and the translucent fibril pellet then resuspended in an equal volume of H_2O. This washing step effectively eliminated most amorphous material (Fig. S5*B*). A solution of F1 monomer was prepared in an identical manner to that detailed above for the F0 generation. The F0 seed was then added to 2% (v/v), and the reaction incubated at 310 K with vigorous stirring for 12–24 hr, resulting in a high yield of fibrils containing significantly less amorphous material (Fig. S5*C*).

Quantitation of fibril binding by centrifugation and intrinsic fluorescence

F1 A53T fibrils were prepared at 70 μM in PBS, and were incubated at room temperature for 1 hr either alone, or with 50 μM αB-crystallin, GFP, or ubiquitin hydrolase (UCH-L3). The samples were centrifuged for 30 min at $16000 \times g$, the supernatants were removed and stored, and the fibril pellets were washed by gently adding an equal volume of PBS buffer and immediately removing it, then resuspending in an equal volume of fresh PBS buffer. SDS-PAGE analysis of supernatant and pelleted fractions was performed on 4–12% Bis-Tris NuPAGE gels in NuPAGE MES SDS running buffer and NuPAGE LDS sample buffer (Invitrogen).

In a second experiment, samples were prepared containing 25 or 50 μM F1 A53T fibrils in PBS and 49 μM αB-crystallin, and were incubated for 1 hr at room temperature prior to centrifugation for 30 min at $16000 \times g$. The intrinsic tryptophan fluorescence of the supernatants were measured using a Cary Eclipse fluorescence spectrophotometer (Varian, UK) with excitation at 275 nm and emission measured at 1 nm intervals from 300 to 500 nm with 1 s averaging. Control spectra were also recorded of 35 μM αSyn monomer and 35 μM αB-crystallin, in isolation and in combination.

NMR spectroscopy

All NMR spectra were recorded on a Bruker Avance 500 MHz TCI-ATM spectrometer equipped with a cryogenic probe. 2D spectra were recorded using uniformly ^{15}N-labelled αSyn (100 μM) at 283 K in PBS with 10% D_2O. [^{1}H,^{15}N]-HSQC spectra were collected with 256 t_1 increments and 16 scans per increment, with sweep widths of 5000 Hz and 1520 Hz in the direct and indirect dimensions respectively, and were processed with NMRPipe (3) using previously reported assignments (2).

1D spectra were recorded at 300 K on three samples: (A) 70 μM F1 A53T fibrils; (B) 20 μM αB-crystallin; and (C) 70 μM F1 A53T fibrils plus 20 μM αB-crystallin. All samples were in PBS buffer, 80% D_2O with 10 μM DSS as an internal reference. DSS has previously been reported to interact with Aβ1–40 and induce oligomerisation (4), upon which a broadening of the DSS resonance was observed; however, the sharp lineshape observed in Fig. 4*A* indicated that there was no such oligomer-inducing interaction with αSyn. Samples A and C were incubated for 12 hr prior to measurement in order that the residual monomer concentration was equilibrated, and this was confirmed by overlaying 1D spectra recorded 4 hr apart. Pulsed-field gradient (PFG) NMR experiments were recorded as 1D and pseudo-1D spectra using bipolar gradient pulses and a 3–9–19 water suppression filter.

Seeded elongation kinetics

F1 A53T fibrils (70 μM) were prepared as described above for use as seed. To ensure a constant fibril end concentration, all measurements were performed simultaneously in black 384 well polystyrene microplates (Nunc) using a FLUOstar fluorescence platereader (BMG Labtech, UK). Samples were prepared with varying concentrations of αB-crystallin and αSyn fibril seed, and 35 μM A53T αSyn in PBS with 20 μM ThT, incubated at 310 K with minimal agitation, and the ThT fluorescence was measured at regular intervals, with excitation at 440 nm and emission at 480 nm. Using Prism (GraphPad Software, La Jolla, USA), data were globally fitted to a sigmoidal dose-response curve as functions of both the absolute concentration of αB-crystallin and of the fibril:chaperone ratio. To investigate the effect of bound αB-crystallin on the fibril seeding efficiency, F1 A53T fibrils (70 μM) were incubated for 1 hr with 70 μM αB-crystallin at room temperature, centrifuged for 30 min at $16000 \times g$, and the fibril pellet was then washed by gently adding an equal volume of PBS buffer and immediately removing it, prior to resuspension in an equal volume of PBS buffer. Control samples containing 70 μM αB-crystallin or 70 μM fibrils were similarly processed. Each sample was then added at 2.5% (v/v) to a 35 μM solution of A53T monomer, and the aggregation kinetics were determined as described above.

QCM

QSX 301 gold-coated sensor crystals were purchased from Q-Sense (Västra Frölunda, Sweden). As αSyn fibrils did not adsorb directly onto the gold surface (Fig. S5*D*), chemistry was required to covalently attach the seed fibrils onto the sensor crystal. An initial approach (described in Supplementary Material) attempted to activate and thiolate aspartate and glutamate sidechains. αSyn fibrils could be attached reliably and cleanly to the sensor surface by this method (Fig. S5*E*). However, while the fibrils were able to elongate, amorphous aggregation was also nucleated at the modified surfaces (Fig. S5*F*). A second more

successful approach, used frequently for the preparation of SPR biosensors (5), minimised the perturbations to the fibril and instead covalently modified and activated the gold surface directly. A gold surface or QCM sensor was incubated in ethanolic 10 mM MUA (11-mercaptoundecanoic acid) overnight in order to form a self-assembled monolayer on the surface. F1 fibrils were freshly prepared with 70 μM A53T αSyn as described above, centrifuged for 60 min at $16000 \times g$ then the supernatant was carefully removed and the pellet resuspended in an equal volume of H_2O. Fibrils were sonicated as necessary (typically 5 min, determined by AFM imaging) to optimise the distribution of lengths on the sensor surface. MUA-coated gold surfaces were rinsed with copious ethanol then H_2O, then loaded with a freshly-prepared solution of 0.4 M 1-ethyl-3-(3-dimethylaminopropyl)carbodiimide hydrochloride, 0.1 M N-hydroxysuccinimide in 50 mM sodium phosphate buffer, pH 6.5. This was allowed to react for exactly 30 min at room temperature then the solution was washed off with copious H_2O, and the surface loaded with the solution of F1 fibrils, which were vortexed briefly for 10 s immediately beforehand to ensure an even dispersion on the surface. The surface was incubated for 4 hr at room temperature in a humidified environment. Excess fibrils were washed off with repeated applications of H_2O for several seconds at a time, and the surface was loaded with 10 mM ethanolamine, pH 9.0, reacted for 1 hr to passivate the remaining surface and finally rinsed with copious H_2O. Once fibrils were attached, the surface was not allowed to dry, as this was observed to inhibit further elongation. Sensor crystals thus prepared were mounted in a Q-Sense D300 QCM, and elongation kinetics were determined as previously described (6).

Immunoelectron microscopy

The chaperone–fibril complex was obtained by the addition of αB-crystallin to F1 A53T αSyn fibrils in PBS, pH 7.5, with final concentrations of 20 μM and 63 μM respectively. The mixture was incubated for 1 hr at room temperature and then spun at $16000 \times g$ for 30 min. The supernatant was carefully aspirated and the pellet resuspended in one volume of PBS, prior to dilution for immunogold labelling as required. Charged carbon-coated nickel electron microscopy grids (400 mesh; Agar Scientific, UK) were prepared for this study by the addition of 4 μL of a 100-fold dilution of the fibril-chaperone complex in PBS (final concentrations 60 nM αSyn and 20 nM αB-crystallin). Samples were deposited onto grids immediately following dilution. Grids were thrice washed with 10 μL H_2O for a few seconds each time, blocked with 15 μL 0.1% (w/v) bovine serum albumin (BSA) in PBS for 15 min, then incubated for 30 min with the αB-crystallin monoclonal primary antibody (100 μg mL^{-1}, Assay Designs) diluted 250-fold in 0.1% BSA in PBS. The grids were blotted with filter paper between each washing step. Next, the grids were thrice washed with 50 μL 0.1% BSA in PBS, for 4 min each time, before a 30 min incubation with goat anti-mouse 10 nm immunogold conjugate (GMHL10, BBInternational), diluted 150-fold into 0.1% BSA in PBS. The grids were then washed with 3×50 μL 0.1% BSA in PBS, again for 4 min each time, then 3×50 μL H_2O for a few seconds each time, and negatively stained with 20 μL of uranyl acetate (2% (w/v) in H_2O); Agar Scientific, UK). Immunogold labelling was performed at room temperature. Samples were viewed under 20–80k magnifications at 80 kV excitation voltages using a Philips CM100 transmission electron microscope.

AFM

AFM imaging of QCM sensor crystals and mica surfaces (Agar Scientific, UK) was performed with a Molecular Imaging Pico Plus atomic force microscope operating in tapping mode, using Ultrasharp silicon cantilevers with a 10 nm tip radius (NCS36, Micromasch, Estonia).

Toy model of αB-crystallin packing on a fibril surface

To estimate the maximum possible amount of binding of αB-crystallin to αSyn fibrils on the basis only of the accessible fibril surface area, it is first necessary to estimate the surface area exposed by a monomer of αSyn within a fibril, $A_{\alpha\text{Syn}}$, and also the area required by αB-crystallin for binding, A_{cryst}. Modelling the fibril as a perfect cylinder, the former is readily determined to be 9.1 ± 2.1 nm^2, given a mean fibril diameter of 7.7 ± 1.7 nm determined by AFM (Fig. 3*A*), and a constant partial specific volume of 0.73 cm^3 g^{-1} (7).

A geometric argument may be developed to estimate the fibril surface area required for the binding of a single αB-crystallin monomer (Fig. S6). For a spherical αB-crystallin monomer with radius r, the half-angle θ subtended by its projection onto the fibril surface (where the fibril is a cylinder with radius R) is $\theta = \sin^{-1}[r/(R+r)]$ and the corresponding arc length r' (Fig. S6) is $r' = R\theta = R\sin^{-1}[r/(R+r)]$. Thus, the projection approximately defines an ellipse on the fibril surface, with area

$$A_{\text{cryst}} = \pi r R \sin^{-1}\frac{r}{R+r}\,. \tag{1}$$

As the three-dimensional structure of αB-crystallin monomer is presently undetermined, an approximate radius of 2.1 nm was estimated using a scaling relationship previously determined for a series of folded proteins (8). This corresponds to $\theta = 20.7^\circ$, and $A_{\text{cryst}} = 9.2$ nm^2. The maximum packing fraction of circles or ellipses on a plane, however, is $\phi = \frac{\pi}{\sqrt{12}} \approx 0.907$ (9). Therefore, the maximum possible binding ratio may be estimated:

$$(\text{cryst} : \alpha\text{Syn})_{\text{max}} = \phi\frac{A_{\alpha\text{Syn}}}{A_{\text{cryst}}} = 0.90 \pm 0.29\,. \tag{2}$$

Attachment of αSyn fibrils to a gold surface by activation of acidic sidechains

F1 A53T fibrils were freshly prepared from 70 μM αSyn monomer as described in the main text, centrifuged for 60 min at $13000 \times g$, and the pellet was resuspended in an equal volume of reaction buffer: 50 mM sodium phosphate buffer, pH 6.5, 2.5 mM EDC (1-ethyl-3-3(3-dimethylaminopropyl) carbodiimide hydrochloride) and 25 mM cystamine. EDC was freshly prepared for each reaction, due to its facile hydrolysis. The resuspended fibrils were reacted for 30 min at room temperature, centrifuged for 40 min at $13000 \times g$, resuspended in an equal volume of H_2O, and the pelleting was repeated one further time to reduce the concentration of free cystamine. The thiolated fibrils thus prepared were vortexed for 10 s and immediately loaded onto the gold surface and reacted for 30 min before washing with copious H_2O. Once fibrils were attached (Fig. S5*E*), the surface was not allowed to dry, as this was observed to inhibit further elongation. However, while fibrils prepared in this manner were able to elongate, amorphous aggregation was also observed to be nucleated on the surface of the modified fibrils (Fig. S5*F*), and for this reason alternative attachment chemistries were explored, as described in the main text.

References

1. Meehan, S., T. P. J. Knowles, A. J. Baldwin, J. F. Smith, A. M. Squires, P. Clements, T. M. Treweek, H. Ecroyd, G. G. Tartaglia, M. Vendruscolo, C. E. Macphee, C. M. Dobson, and J. A. Carver, 2007. Characterisation of Amyloid Fibril Formation by Small Heat-shock Chaperone Proteins Human alphaA-, alphaB- and R120G alphaB-Crystallins. *J. Mol. Biol.* 372:470–484.

2. Dedmon, M. M., J. Christodoulou, M. R. Wilson, and C. M. Dobson, 2005. Heat shock protein 70 inhibits alpha-synuclein fibril formation via preferential binding to prefibrillar species. *J. Biol. Chem.* 280:14733–14740.

3. Delaglio, F., S. Grzesiek, G. W. Vuister, G. Zhu, J. Pfeifer, and A. Bax, 1995. NMRPipe: a multidimensional spectral processing system based on UNIX pipes. *J. Biomol. NMR* 6:277–293.

4. Laurents, D. V., P. M. Gorman, M. Guo, M. Rico, A. Chakrabartty, and M. Bruix, 2005. Alzheimer's Abeta40 studied by NMR at low pH reveals that sodium 4,4-dimethyl-4-silapentane-1-sulfonate (DSS) binds and promotes beta-ball oligomerization. *J. Biol. Chem.* 280:3675–3685.

5. Hasegawa, K., K. Ono, M. Yamada, and H. Naiki, 2002. Kinetic modeling and determination of reaction constants of Alzheimer's beta-amyloid fibril extension and dissociation using surface plasmon resonance. *Biochemistry* 41:13489–13498.

6. Knowles, T. P. J., W. Shu, G. L. Devlin, S. Meehan, S. Auer, C. M. Dobson, and M. E. Welland, 2007. Kinetics and thermodynamics of amyloid formation from direct measurements of fluctuations in fibril mass. *Proc. Natl. Acad. Sci. USA* 104:10016–10021.

7. Baldwin, A. J., R. Bader, J. Christodoulou, C. E. MacPhee, C. M. Dobson, and P. D. Barker, 2006. Cytochrome display on amyloid fibrils. *J. Am. Chem. Soc.* 128:2162–2163.

8. Wilkins, D. K., S. B. Grimshaw, V. Receveur, C. M. Dobson, J. A. Jones, and L. J. Smith, 1999. Hydrodynamic radii of native and denatured proteins measured by pulse field gradient NMR techniques. *Biochemistry* 38:16424–16431.

9. Pach, J., and P. K. Agarwal, 1995. Combinatorial Geometry. Wiley-Interscience, 1st edition.

Supporting Material: Figure Captions

Figure S1 — Analysis of SDS-PAGE and the sedimentation of isolated αB-crystallin. (A) Densitometric analysis of Fig. 1*A*, showing the relative abundance of proteins in pellets 1–4. Peaks were integrated and normalised by protein mass, to determine the approximate ratios of 56% αB-crystallin, 8% GFP and 1% UCH-L3 relative to αSyn. (B) SDS-PAGE showing 50 μM αB-crystallin, and the supernatant following centrifugation at $16000 \times g$ for 30 min. (C) Densitometric analysis of the digitised electrophoretogram. The integrals of both peaks were identical within measurement error.

Figure S2 — αSyn monomer NMR chemical shift perturbations. The reported change in chemical shift for a 100 μM sample of WT ^{1}H,^{15}N-αSyn is a normalised combination of HN and N shifts, $\Delta\delta = \sqrt{\Delta\delta_H^2 + (\Delta\delta_N/10)^2}$, following the addition of 1 equivalent of αB-crystallin. The perturbation at His50 (*) may be attributed to its high sensitivity to small changes in pH.

Figure S3 — QCM determination of the concentration dependence of αSyn fibril elongation. Kinetics were determined using A53T αSyn monomer in PBS at 300 K.

Figure S4 — NMR characterisation of diffusion in a solution of αSyn fibrils. (A) Methyl proton signal intensity of a 70 μM solution of αSyn fibrils in a 1D PFG NMR experiment, as a function of the applied gradient strength ($G_{\%}^2$, where $G_{\%}$ is the fraction of the maximum field strength, 34.6 T cm^{-1}) and of the diffusion delay Δ. Lines show fits to the Stejskal-Tanner equation. (B) Effective diffusion constants calculated from the fits in (A), and also for similar fits to two separate peaks, as a function of the diffusion delay Δ.

Figure S5 — AFM imaging of αSyn fibril preparations on mica and gold surfaces. (A) First-generation A53T fibrils; (B) first-generation fibrils pelleted and resuspended in H_2O; (C) second-generation fibrils, pelleted and resuspended in H_2O at the same nominal concentration as (B). (D) Unmodified gold surface following incubation with second-generation fibrils. (E) Thiolated A53T fibrils covalently attached to a gold surface, as described in Supplementary Material. (F) Mixed fibrillar and amorphous growth of thiolated αSyn fibrils on a gold surface.

Figure S6 — Geometric analysis of αB-crystallin packing on a fibril surface. The fibril and chaperone cross-sections are drawn to scale, with diameters of 7.7 and 4.2 nm respectively, as described in the Methods section.

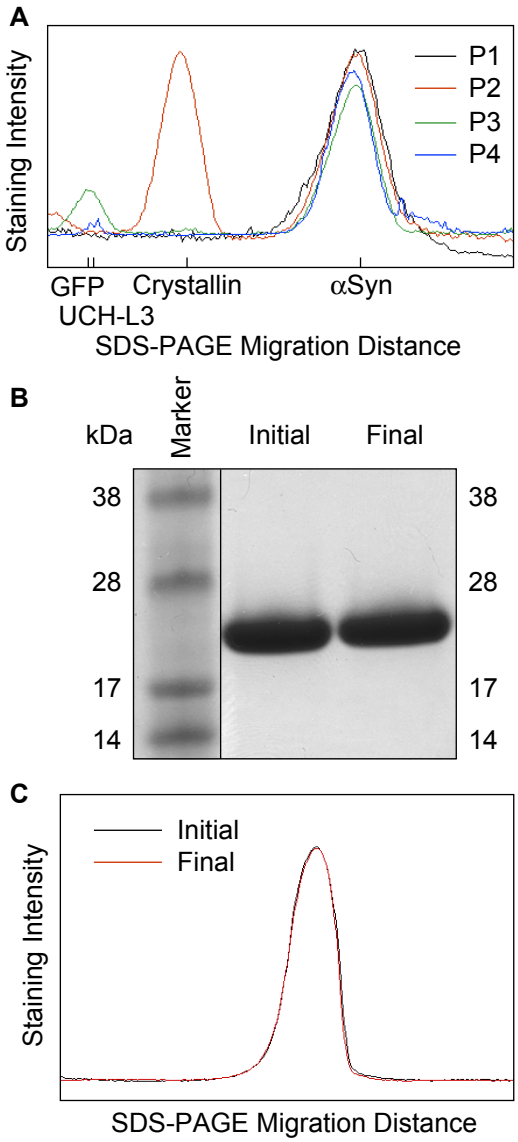
A
Staining Intensity
P1
P2
P3
P4
GFP
UCH-L3
Crystallin
αSyn
SDS-PAGE Migration Distance
B
kDa
Marker
Initial
Final
38
28
17
14
38
28
17
14
C
Staining Intensity
Initial
Final
SDS-PAGE Migration Distance

Figure 1

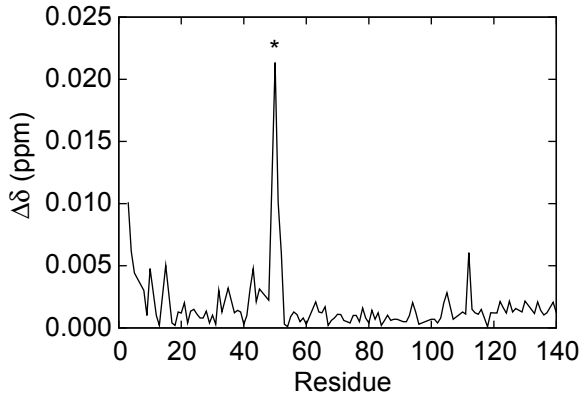
0.025
0.020
0.015
0.010
0.005
0.000
Δδ (ppm)
*
0
20
40
60
80
100
120
140
Residue

Figure 2

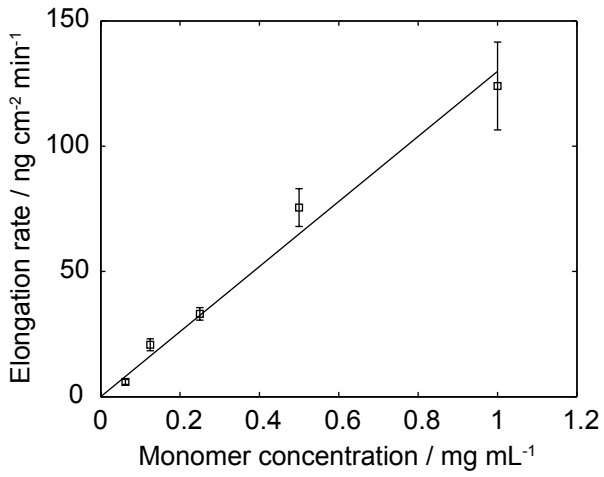
150
100
50
0
0
0.2
0.4
0.6
0.8
1
1.2
Elongation rate / ng cm-2 min-1
Monomer concentration / mg mL-1

Figure 3

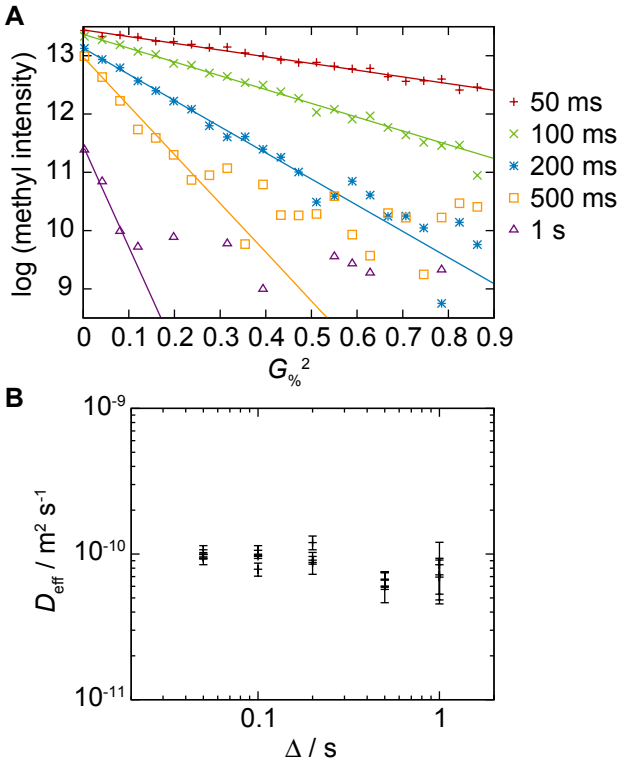
A
log (methyl intensity)
13
12
11
10
9
0 0.1 0.2 0.3 0.4 0.5 0.6 0.7 0.8 0.9
$G_{\%}^2$
50 ms
100 ms
200 ms
500 ms
1 s
B
D_{eff} / m^2 s^{-1}
10^{-9}
10^{-10}
10^{-11}
0.1
1
Δ / s

Figure 4

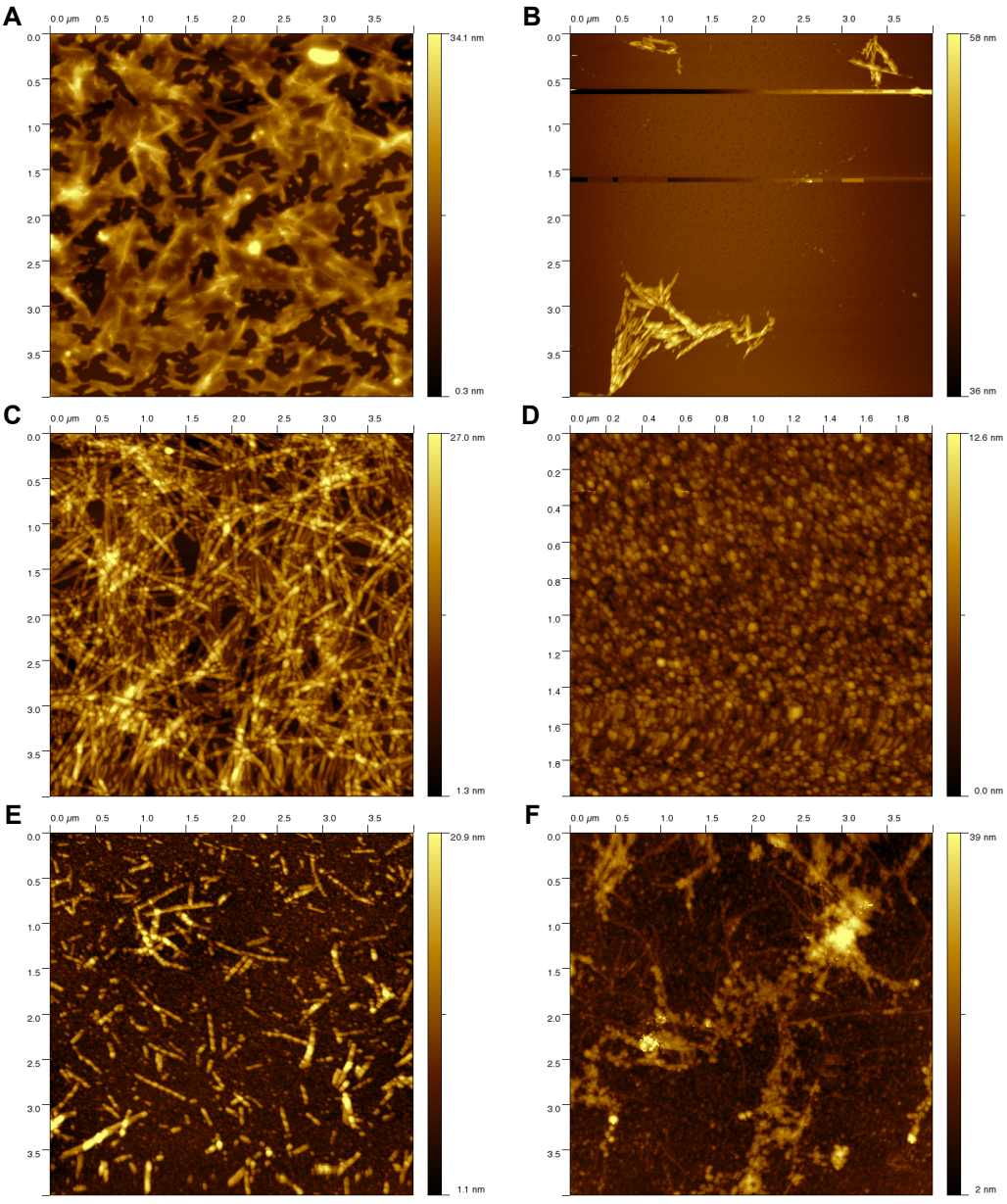
A
B
C
D
E
F
34.1 nm
0.3 nm
58 nm
36 nm
27.0 nm
1.3 nm
12.6 nm
0.0 nm
20.9 nm
1.1 nm
39 nm
2 nm

Figure 5

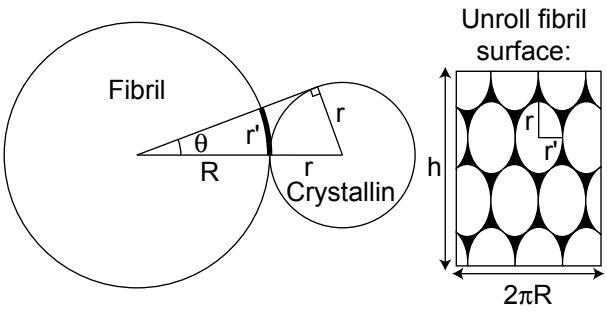

Figure 6